10

Influence of the method of strong doping on composition uniformity and optical properties of $LiNbO_3:Mg$ single crystals

© N.V. Sidorov, H.A. Teplyakova ¶, M.H. Palatnikov

Tananaev Institute of Chemistry Subdivision of the Federal Research Centre „Kola Science Centre of the Russian Academy of Sciences", Apatity, Russia

¶ e-mail: n.tepliakova@ksc.ru

Received June 09, 2021
Revised June 09, 2021
Accepted June 23, 2021

Raman spectroscopy, laser conoscopy and photoinduced light scattering methods have been applied to comparatively study composition uniformity of strongly doped $LiNbO_3$ crystals with a magnesium concentration close to a threshold value ≈ 5 mol% MgO, grown from a charge synthesized using precursor $Nb_2O_5:Mg$ (homogeneous doping method) and at direct addition of magnesium to the melt (direct doping method). It has been shown that application of homogeneous doping method allows one to obtain compositionally more homogeneous heavily doped $LiNbO_3:Mg$ crystal than direct melt doping method.

Keywords: lithium niobate crystal, homogeneous and direct doping, Raman scattering, laser conoscopy, photoinduced light scattering.

DOI: 10.21883/EOS.2022.01.53003.13-21

Introduction

Nonlinear optical photorefractive lithium niobate crystal ($LiNbO_3$) is one of the most important materials of acoustic and optoelectronics, integrated and laser optics. At present, there is a high demand for functional nonlinear optical materials based on $LiNbO_3$ single crystal of high compositional homogeneity with a low photorefraction effect and a coercive field. The photorefraction effect and the magnitude of the coercive field in $LiNbO_3$ crystal can be most significantly reduced by doping with high (close to a second concentration threshold and higher) concentrations of metals Mg^{2+}, Zn^{2+}, Gd^{3+} etc. [1,2]. At some „threshold" concentrations (constant for each impurity), all concentration dependences of properties reveal abnormalities [2]. In particular, for $LiNbO_3:Mg$ crystal two concentration thresholds were found at ≈ 3 and 5.5 mol% MgO, at which an abrupt change in the defect state and physical characteristics of the crystal is observed [2]. Thus, an introduction to a congruent ($R = Li/Nb = 0.946$) $LiNbO_3$MgO crystal in the amount of ≈ 5 mol% (concentration threshold is ≈ 5.5 mol% MgO) reduces the coercive field from 22–23 kW/mm to 4.8 kW/mm, which is very important for creating nonlinear optical single crystal materials with periodically polarized domains for laser radiation conversion [3–6]. However, with such heavy doping (due to the nonuniform distribution over the crystal volume of the dopant and associated point and complex defects), the composition inhomogeneity of the single crystal increases significantly thus reducing the homogeneity of many physical characteristics of the material. The coefficient of metals Mg^{2+}, Zn^{2+}, etc. inclusion in the structure of $LiNbO_3$ crystal and its composition homogeneity are also significantly affected by the method of doping [1].

Determination how the dopant and the method of doping affect the composition homogeneity and optical properties of the $LiNbO_3$ single crystal, in view of its wide application as a functional nonlinear optical material, is an urgent task of great practical importance.

Papers [1,7–12] show the comparative studies of the structural features and optical properties of some compositions of $LiNbO_3:Mg$ crystals obtained by the Czochralski method carried out in two ways: by direct doping of the melt (used in industry), when the dopant is introduced directly into the melt before melting the crucible, and by a new method [13] comprising a charge synthesized using the $Nb_2O_5:Mg$ precursor (homogeneous doping method). It is logical to assume that clusters and complexes consisting of octahedral $(Nb(Mg)O_6)$ and tetrahedral $(Nb(Mg)O_4)$ structures [14–18], existing in melts of $Nb_2O_5:Li_2O$ and $Nb_2O_5:Li_2O:MgO$ systems and forming the composition homogeneity of the $LiNbO_3$ crystal differ in structure, size, and chemical activity. Consequently, melts having different composition and doping method, and under other equal conditions should crystallize differently with the formation of different composition homogeneity of the crystal [14,15]. Indeed, studies of the macro- and microstructural homogeneity of doped $LiNbO_3:Mg$ crystals by optical methods indicate a higher composition homogeneity of some homogeneously doped crystals compared to direct-doped crystals [7–12]. In particular, when using the method of homogeneous doping, there are fewer defects in the crystal in the form of growth bands, dislocations, clusters and microstructures, microdomains, domain boundaries and block-like structures inherent to the direct doped crystals [1,19,20].

This can presumably be explained by the fact that during homogeneous doping, the alloying element Me (Me = Mg, Zn, Gd, etc.) even at the stage of Nb_2O_5 : Me precursor synthesis forms mainly intraoctahedral coordination with a more uniformly distribution over the melt volume, which increases the concentration of $Nb(Me)O_6$ clusters with an oxygen-octahedral structure in the melt and the coefficient of metal incorporation into the structure of the $LiNbO_3$ crystal, making the crystal more compositionally homogeneous. The estimated effective magnesium distribution coefficient for the homogeneous doping method is ≈ 1.17. In the direct melt doping method, magnesium has a lower distribution coefficient (≈ 1.11) [1].

This paper presents the results of comparative complex studies using Raman spectroscopy (RSS), photoinduced light scattering (PILS) and laser conoscopy of composition homogeneity and some optical properties of close in composition heavily doped monodomainized crystals $LiNbO_3$: Mg (5.03 mol% MgO) and $LiNbO_3$: Mg (4.75 mol% MgO), obtained respectively by the method of direct doping of the melt and by the method of homogeneous doping from the charge synthesized using the Nb_2O_5 : Mg precursor.

Experimental procedure

The production of $LiNbO_3$: Mg single crystals of different compositions by direct doping of the melt and by the method of homogeneous doping using the Nb_2O_5 : Mg precursor is described in detail in the papers [1,8–12]. The crystals were grown in an air by the Czochralski method on „Kristall-2“unit. The grown single crystals were monodomainized by high-temperature electrodiffusion annealing with direct current application while cooling the crystals at a rate of 20 grad/h in the temperature range of $\sim 1240-880^\circ$C. The degree of monodomain was monitored by analyzing the frequency dependence of the electrical impedance and by determining the value of the static piezoelectric modulus (d_{333st}) of the crystal boule. Samples for studies were prepared from monodomainized crystals in the form of parallelepipeds ($7 \times 6 \times 5$ mm), the edges of which coincided in direction with the crystallophysical axes X, Y, Z, respectively (Z is the polar axis of the crystal). The faces of the parallelepipeds were thoroughly polished.

The RSS spectra were excited by 514.5 nm line of Spectra Physics argon-krypton laser (model 2018-RM) and recorded with T64000 spectrograph (Horiba Jobin Yvon) using a confocal microscope. To reduce the photorefraction effect on the RSS spectrum, the spectra were excited by low-power radiation (3 mW). All spectra were recorded with a resolution of 1.0 cm^{-1}. The spectra were processed using the Horiba LabSpec 5.0 and Origin 8.1 programs package. The accuracy of determining the frequencies, widths and intensities of ± 1.0, ± 3.0 cm^{-1} and 5% lines, respectively. Details of the research methods as PILS and laser conoscopy are given in the paper [21]. In PILS and laser conoscopy experiments Nd : YAG (MLL-100) laser with a generation line of 532 nm and a power of up to 160 mW, $d = 1.8$ mm was used. To assess the composition homogeneity of crystals, PILS conoscopic patterns and RSS spectra in various polarization geometries were recorded with a step of 5 mm from different points of the studied crystals.

Results and discussion

RSS spectra of single crystals $LiNbO_{3cong}$, $LiNbO_3$: Mg (4.75 mol% MgO, homogeneous doping) and $LiNbO_3$: Mg (5.03 mol% MgO, direct doping) recorded in the range of $50-1000$ cm^{-1} in the backscattering geometry $Y(ZZ)\bar{Y}$ and $Y(ZX)\bar{Y}$ (in Porto notation [22] are active, respectively, fundamental vibrations of A_1(TO) and E(TO) symmetry types [2]) in polarized radiation are shown in Fig. 1. RSS spectra of polycrystals $LiNbO_{3cong}$, Nb_2O_5 and Nb_2O_5 : Mg (5.54 mol% MgO) are shown in Fig. 2. In RSS spectrum of oxygen-octahedron crystal structures of $LiNbO_3$ and Nb_2O_5 in the range of $150-400$ cm^{-1} predominantly lines corresponding to fundamental vibrations of intraoctahedral cations (Li, Nb, Mg) in the range of $550-1000$ cm^{-1} — vibrations of the oxygen frame of the crystal [2,23] occur. At the same time, in the range of $850-950$ cm^{-1}, stretching bridged vibrations (SBV) of oxygen atoms along the polar axis in the bridge Me−O−Me (Me−Nb, Li, impurity metal) are observed, they are most sensitive to changes in the polarizability of the oxygen-octahedral clusters MeO_6 [2,23]. When the oxygen-octahedral structure is destroyed with the formation of island structures of O_6 octahedrons, Me−O−Me bridge is destroyed, and lines corresponding to the end vibrations of Me−O, whose frequency is higher than the SBV frequencies of oxygen atoms along the polar axis [23], occur. SBV of oxygen atoms along the polar axis in the Me−O−Me bridge are active in the RSS spectrum only for noncentrosymmetric oxygen-octahedral MeO_6 clusters [23]. It should be noted that the RSS spectrum of a pure Nb_2O_5 polycrystal is represented by a smaller number of lines than the spectrum of the polycrystal Nb_2O_5 : Mg (5.54 mol% MgO, homogeneous doping), Fig. 2.

Frequencies and widths of experimentally observed lines in the RSS spectra of $LiNbO_{3cong}$, $LiNbO_3$: Mg single crystals and line frequencies in the spectra of Nb_2O_5 and Nb_2O_5 : Mg polycrystals are shown in the Table. It turned out to be impossible to correctly determine the linewidths in the spectrum of Nb_2O_5 and Nb_2O_5 : Mg polycrystals due to the large overlapping of the lines (Fig. 2). Nb_2O_5, like $LiNbO_3$ has a region of homogeneity in the phase diagram and is a phase of variable composition. At the same time, in contrast to the $LiNbO_3$ crystal, in which only two polymorphic modifications (low-temperature ferroelectric and high-temperature paraelectric, $T_c \approx 1480$ K), and both have oxygen-octahedral structure, at least fifteen polymorphic modifications are known for crystalline niobium pentoxide,

Main parameters of the RSS spectra lines of single crystals $LiNbO_{3cong}$ and $LiNbO_3:Mg$ (homogeneous and direct doping) in scattering geometries $Y(ZX)\bar{Y}$ (oscillations of E(TO) symmetry type are active) and $Y(ZZ)\bar{Y}$ (oscillations of A_1(TO) symmetry type are active);$P = 3$ mW; $\lambda_0 = 514.5$ nm

$LiNbO_{3cong}$		$LiNbO_3:Mg$ (4.75 mol% MgO) (homogeneous doping)		$LiNbO_3:Mg$ (5.03 mol% MgO) (direct doping)	
ν, cm^{-1}	S, cm^{-1}	ν, cm^{-1}	S, cm^{-1}	ν, cm^{-1}	S, cm^{-1}
$Y(ZX)\bar{Y}$, E(TO)					
152	12	157	12	157	11
240	11	249	12	249	12
268	14	274	18	274	18
324	13	331	20	330	19
371	23	375	28	375	28
434	14	439	17	439	17
576	15	576	28	576	27
$Y(ZZ)\bar{Y}$, A_1(TO)					
254	30	265	21	265	22
275	12	281	19	282	19
332	11	337	15	338	16
631	26	626	31	625	30

and only insignificant part of them has oxygen-octahedral structure [24–29]. The most common modifications of Nb_2O_5 are monoclinic α-form, hexagonal β-form and orthorhombic γ-form. The RSS spectra of mixture of some Nb_2O_5 modifications were studied in papers [24,26–29]. To obtain the single crystal of high composition homogeneity, it is important that, during the synthesis of a lithium niobate charge, the Nb_2O_5 and $Nb_2O_5:Mg$ precursors be single-phase in maximum extent, and, like $LiNbO_3$ charge, have predominantly oxygen-octahedral structure.

The RSS spectrum of Nb_2O_5 and $Nb_2O_5:Mg$ polycrystals used by us to synthesize the lithium niobate charge, in SBV area of oxygen atoms has five lines with frequencies of 814, 845, 902, 965, 995 cm^{-1} (Fig. 2), which indicates the presence of both oxygen-octahedral and oxygen-tetrahedral island structures consisting of chain fragments of $Nb(Mg)O_6$ octahedrons and $Nb(Mg)O_4$ tetrahedrons. In this case, the line with frequency of 845 cm^{-1} corresponds to the SBV of oxygen atoms of Nb–O–Nb in tetrahedral clusters NbO_4, and the line with frequency of 902 cm^{-1} — to the SBV of oxygen atoms in NbO_6 octahedral clusters [23]. The line with frequency of 965 cm^{-1} is attributed to the end stretching vibrations of Nb–O in isolated (island) NbO_4 tetrahedrons, and the line with frequency of 995 cm^{-1} — to end stretching vibrations of Nb–O in isolated (island) octahedrons [23,24]. Significantly lower (in the RSS spectrum of $Nb_2O_5:Mg$ polycrystal) intensities of lines with frequencies of 965 and 995 cm^{-1}, corresponding to the end vibrations of Nb–O in NbO_4 tetrahedrons and NbO_6 octahedrons (Fig. 2), indicate a smaller number of isolated island structures in $Nb_2O_5:Mg$ precursor than in the structure of pure Nb_2O_5. That is, the concentration of phases with oxygen-octahedral structure is higher in $Nb_2O_5:Mg$ precursor (homogeneous doping) than in pure Nb_2O_5.

The line frequencies in the RSS spectra of $LiNbO_3:Mg$ single crystals of homogeneous and direct doping, corresponding to vibrations of E(TO) and A_1(TO) symmetry types, are in good agreement with each other and noticeably differ from the corresponding frequencies in spectrum of $LiNbO_{3cong}$ crystal, (Table), which indicates a noticeable difference between the corresponding quasi-elastic immutable bindings in nominally pure and magnesium-doped $LiNbO_3$ crystals. Almost all lines in the spectrum of doped crystals are much wider than in the spectrum of nominally pure $LiNbO_3$ crystal, which indicates an increased disorder in the arrangement of structural units of the cationic sublattice and a greater „exciting“ of O_6 oxygen octahedrons of doped crystals as compared with the octahedrons of nominally pure $LiNbO_3$ crystal. Moreover, like the line frequencies, the corresponding linewidths are close in the spectra of doped crystals and differ greatly from the corresponding linewidths in the spectrum of the $LiNbO_{3cong}$ crystal. Especially large widening (almost by two times) is observed in the line with frequency of 576 cm^{-1}, which corresponds to doubly degenerated vibrations of oxygen

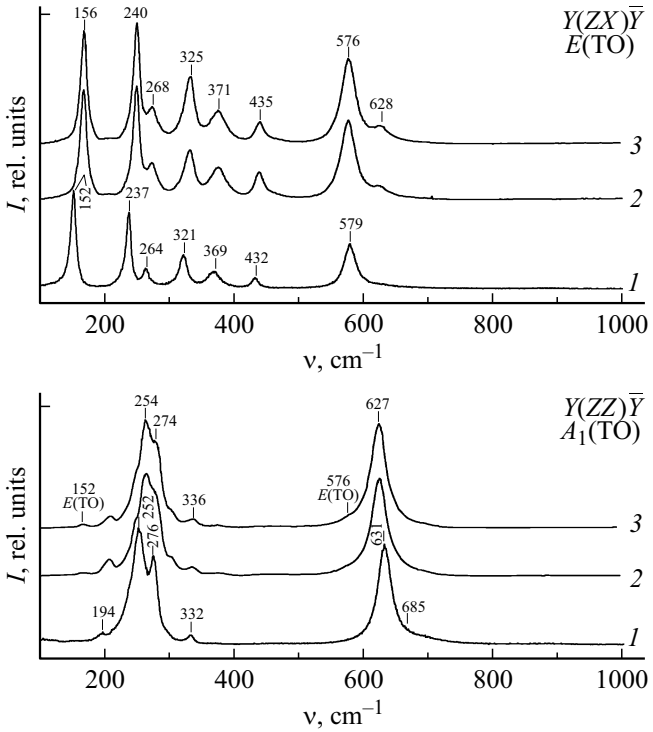

Figure 1. RSS spectra of $LiNbO_{3cong}$ single crystals (curve *1*), $LiNbO_3:Mg$ (5.03 mol% MgO, direct doping, curve *2*), $LiNbO_3:Mg$ (4.75 mol% MgO, homogeneous doping, curve *3*), in scattering geometries $Y(ZX)Y$ and $Y(ZZ)Y$; $P = 3$ mW; $\lambda_0 = 514.5$ nm. $T = 293$ K.

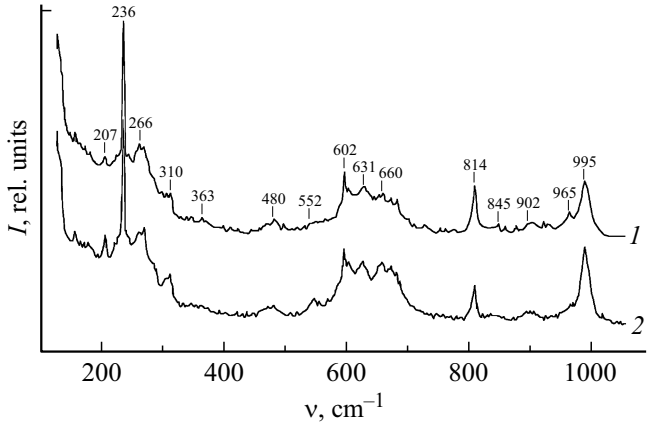

Figure 2. RSS spectra of polycrystalline samples: curve *1* — $Nb_2O_5:Mg$ (5.54 mol% MgO, homogeneous doping), *2* — Nb_2O_5.

atoms of E(TO) symmetry type occurring perpendicular to the polar axis of the crystal. In this case, the line with frequency of 631 cm^{-1} ($LiNbO_{3cong}$) corresponding to „breathing“ vibrations of $A_1(TO)$ symmetry type of O_6 oxygen octahedrons is widened much less significantly. This fact indicates a noticeable „excitation“ (expansion) by magnesium of O_6 oxygen octahedrons due to length change in the O−O bonds.

It is unusual that in the low-frequency region of the RSS spectrum, where vibrations of intraoctahedral cations along and perpendicular to the polar axis are manifested, upon a significant difference in line frequencies in the spectra of the $LiNbO_{3cong}$ crystal and $LiNbO_3:Mg$ crystals (direct and homogeneous doping) the differences in linewidths are small. In this case, the linewidth with frequency of 254 cm^{-1} corresponding to vibrations of $A_1(TO)$ symmetry type of Nb ions along the polar axis, most of all in the spectrum of $LiNbO_{3cong}$ crystal than in the spectra of crystals doped with magnesium. On other hand, linewidth with frequency of 275 cm^{-1} corresponding to vibrations of $A_1(TO)$ symmetry type of Li ions along the polar axis is smaller in the spectrum of $LiNbO_{3cong}$ crystal than in the spectra of crystals doped with magnesium. The narrowing of the line indicates a more ordered state of the lithium sublattice and a more disordered state of the niobium sublattice in $LiNbO_{3cong}$ crystal (characterized by a high concentration of Nb_{Li} point defects) as compared to crystals heavily doped with magnesium. These data confirm the results of papers [2,7,8] that at magnesium concentrations near the concentration threshold of 5.0 mol% MgO, some ordering of the cationic sublattice occurs due to the almost complete replacement by magnesium ions of point defects Nb_{Li}, which are the deepest electron traps in pure $LiNbO_3$ crystal and have a significant influence on the photorefraction effect. Note that in relation to ordering of the defects sublattice from hydrogen atoms the crystals $LiNbO_3:Mg$ (5.03 mol% MgO, direct doping) and $LiNbO_3:Mg$ (4.75 mol% MgO, homogeneous doping) are identical to each other, but noticeably differ from $LiNbO_{3cong}$ crystal. Three lines with frequencies of 3470, 3483, 3486 cm^{-1} are observed in the IR absorption spectrum of the $LiNbO_{3cong}$ crystal in the region of stretching vibrations of OH-groups. While in the IR spectrum of heavily doped crystals $LiNbO_3:Mg$ there are only two lines with significantly higher frequencies: 3526 and 3535 cm^{-1} [7,8]. Such a strong shift of the spectrum to the high-frequency region is due to a decreased number of complex defects $Nb_{Li}-OH$ due to their displacement by magnesium, and the formation of defect complexes $Mg_{Li}-OH$ and $Mg_{Nb}-OH$. In this case, due to the conservation of the electrical neutrality of the crystal, the number of vacant (V) octahedrons O_6 and complex defects $V_{Li}-OH$ associated with them will change.

A specific feature of lithium niobate single crystals doped with relatively high (≥ 3 mol% MgO) magnesium concentrations is the non-uniform entry of the impurity into the crystal [8,10,19,30] and, accordingly, the appearance of growth bands associated with concentration gradients of dopant both in the perpendicular plane and in the plane parallel to the growth axis. The appearance of growth bands is accompanied by the appearance of microdefects in the form of dislocations, microdomains, domain boundaries, and block structure, which are especially noticeable in the region of increased impurity concentration gradients at the boundaries of growth bands [20,30]. It is quite difficult

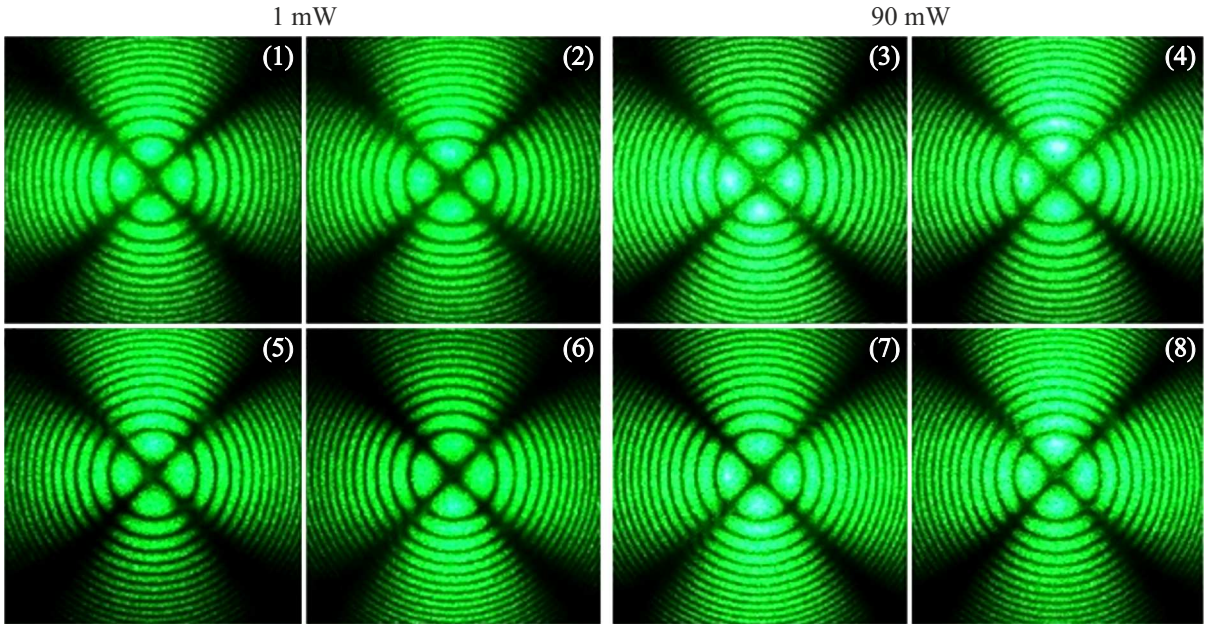

Figure 3. Conoscopic patterns of $LiNbO_3$: Mg crystals of direct (*1–4*) and homogeneous (*5–8*) doping obtained by scanning along the plane of input edge. $\lambda = 532$ nm. $P = 1$ and 90 mW.

to get rid of such defects, since they are an additive result of the physicochemical properties of the melt and the lithium niobate ferroelectric crystal. As a rule, growth rings and bands in doped lithium niobate crystals are the result of impurity segregation. The diffusion-defect structure arising in the latter case is fixed upon cooling from the crystallization temperature to temperature below the Curie point [1].

In papers [16–18], the transition of the crystal structure into melt and melt ($Nb_2O_5-Li_2O$ system) at various temperatures of a nominally pure $LiNbO_3$ crystal was studied by high-temperature RSS spectroscopy. It was shown that in the premelting region of $LiNbO_3$ congruent crystal the rearrangement of its structure begins, as a result of which tetrahedral coordination of niobium atoms appears in the oxygen-octahedral crystalline matrix. The presence of NbO_4 tetrahedrons in the premelting region and in the molten state of $Nb_2O_5-Li_2O$ system is provided by a strong Nb–O covalent bond. Since lithium is bound to oxygen by a much weaker electrostatic interaction, no LiO_4 tetrahedron [16–18] was found in the lithium niobate melt. It was also shown that the melt may contain not only isolated tetrahedral groups, but also other complexes with a stable structure [17,18]. It is also obvious that Mg–O covalent bonds and the corresponding complexes will remain in the melt. Since, as it was already shown above, in the crystal structure of Nb_2O_5 : Mg precursor used, the concentration of phases with octahedral coordination of niobium is higher than in Nb_2O_5 structure, we can expect that homogeneous doped crystals will be characterized by greater composition homogeneity than crystals of direct doped melt.

Previously, in papers [8,9,30] for crystal $LiNbO_3$: Mg (5.03 mol% MgO, direct doping) the clearly pronounced growth bands were found when studying the macro- and microstructure. At the same time, for crystal $LiNbO_3$: Mg (4.75 mol% MgO, homogeneous doping) such macro- and microdefects were absent both for the *X*-cut and for the *Z*-cut [8,9]. Higher composition homogeneity of the crystal $LiNbO_3$: Mg (4.75 mol% MgO, homogeneous doping) in comparison with crystal $LiNbO_3$: Mg (5.03 mol% MgO, direct doping) also confirms the fact that the difference between the MgO concentrations determined by us in the cone and end parts of the boule of crystal $LiNbO_3$: Mg (homogeneous doping) is less than for crystal $LiNbO_3$: Mg (direct doping). For a homogeneous doped crystal it is 0.06 mol% MgO, and for direct doped crystal it is almost by two times higher (0.11 mol% MgO).

One of the most sensitive methods for studying the composition homogeneity of single crystals is the method of laser conoscopy in strongly divergent beams of laser radiation [21]. The appearance of growth bands, impurity concentration gradients, and clusters of microdefects leads to local change in the elastic characteristics of the crystal and the appearance of mechanical stresses [21,30] that locally distort the optical indicatrix of optically uniaxial lithium niobate crystal. The latter must inevitably lead to distortion of the conoscopic patterns. Moreover, the maximum distortion is observed for conoscopic patterns at the boundaries of growth bands, where the concentrations of structural defects and concentration gradients of the dopant are maximum. Conoscopic patterns of crystals $LiNbO_{3cong}$, $LiNbO_3$: Mg (4.75 mol% MgO, homogeneous doping) and $LiNbO_3$: Mg (5.03 mol% MgO, direct doping)

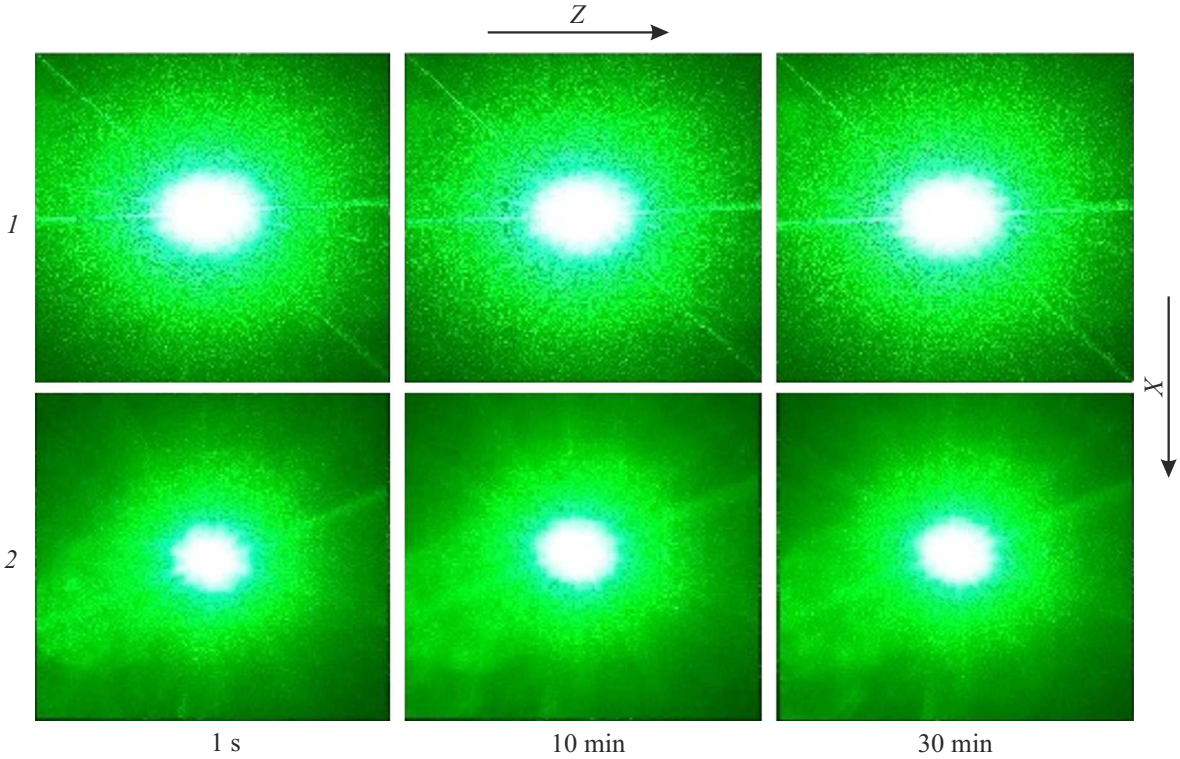

Figure 4. Circular scattering on static structural defects of the structure of crystals $LiNbO_3:Mg$ of direct (*1*) and homogeneous (*2*) doping. $\lambda = 532$ nm. $P = 160$ mW.

obtained at different laser radiation power are shown in Fig. 3. All conoscopic patterns correspond to patterns of uniaxial crystal of high optical uniformity. When the laser radiation power increases to 90 mW, no additional anomalies were found in the conoscopic patterns, which indicates the absence of photoinduced distortions in the crystal structure caused by the action of laser radiation. Like the RSS spectra (Fig. 1), the conoscopic patterns of all three crystals are significantly different. The conoscopic patterns of the crystal $LiNbO_3:Mg$ (4.75 mol% MgO, homogeneous doping) are more perfect (Fig. 3, curves *5*–*8*). They correspond to the patterns of uniaxial crystal of high optical quality. The conoscopic patterns of the crystal $LiNbO_3:Mg$ (5.03 mol% MgO, direct doping) are more blurred (Fig. 3, curves *1*–*4*) in comparison with the pictures of the crystal $LiNbO_3:Mg$ (4.75 mol% MgO, homogeneous doping): on the upper left branch of the „Maltese“ cross the presence of defects, which are obviously related to uneven entry of the magnesium dopant into the crystal structure. It should be noted that when scanning along the plane of the input face for crystal $LiNbO_3:Mg$ (5.03 mol% MgO, direct doping) in contrast to the RSS spectra different conoscopic patterns were obtained (Fig. 3, curves *1*–*4*), which indicates the composition inhomogeneity of this crystal. At the same time, the conoscopic patterns show low signs of anomalous optical biaxiality (Fig. 3, curves *1* and *3*), which is expressed in the deformation of „Maltese“ cross in the vertical direction from the center, corresponding to the direction of deformation of optical indicatrix.

PILS patterns show high resistance of crystals $LiNbO_{3cong}$, $LiNbO_3:Mg$ (4.75 mol% MgO, homogeneous doping) and $LiNbO_3:Mg$ (5.03 mol% MgO, direct doping) to optical damage by laser radiation 160 mW ($I = 6.29$ W/cm^2). It can be seen from Fig. 4 that the speckle structure of the PILS indicatrix of the studied crystals is not discovered, and only circular scattering on static structural defects is observed, which indicates a low photorefraction effect. In this case, the PILS patterns (as well as the conoscopic patterns, Fig. 3) of the studied crystals differ noticeably. The crystal $LiNbO_3:Mg$ (5.03 mol% MgO, direct doping) is characterized by a higher scattering power than the crystal $LiNbO_3:Mg$ (4.75 mol% MgO, homogeneous doping), which indicates its high composition homogeneity.

Conclusion

RSS, PILS and laser conoscopy methods were applied to close in composition heavily doped crystals $LiNbO_3:Mg$ (5.03 mol% MgO) and $LiNbO_3:Mg$ (4.75 mol% MgO) obtained by two ways: by direct doping of melt and by homogeneous doping from a charge synthesized using the $Nb_2O_5:Mg$ precursor. The RSS spectra of $LiNbO_{3cong}$ polycrystals and precursors Nb_2O_5 and $Nb_2O_5:Mg$ (5.54 mol% MgO), from which

$LiNbO_3:Mg$ crystals of direct and homogeneous doping were grown, respectively.

The RSS spectra of $LiNbO_3:Mg$ single crystals of homogeneous and direct doping practically do not differ from each other, but noticeably differ from the spectrum of the $LiNbO_{3cong}$ crystal. RSS data indicate a noticeable „excitation" (expansion) with magnesium of O_6 oxygen octahedrons due to change in the lengths of O–O bonds, but at that the narrowing of the lines in the low-frequency region of the spectrum indicates a more ordered state of the lithium sublattice and a more disordered state of the niobium sublattice in $LiNbO_{3cong}$ crystal (characterized by a high concentration of point defects Nb_{Li}) as compared to crystals that were heavily doped with magnesium.

The results obtained by PILS and laser conoscopy show that the crystal $LiNbO_3:Mg$ (4.75 mol% MgO, homogeneous doping) is characterized by greater optical homogeneity as compared to the crystal $LiNbO_3:Mg$ (5.03 mol% MgO, direct doping). In this case, both crystals $LiNbO_3:Mg$ have low photorefraction effect.

The study of RSS spectra of the precursors showed that the concentration of the phases with the oxygen-octahedral structure is higher in the precursor $Nb_2O_5:Mg$ (5.54 mol% MgO, homogeneous doping) than in pure Nb_2O_5. This fact allows us to conclude that a more uniform distribution of the dopant in homogeneous doped crystals begins to form already at the stage of synthesis of $Nb_2O_5:Mg$ precursor and lithium niobate charge during the formation of chemically active complexes that determine predominantly oxygen-octahedral structure of $Nb_2O_5:Mg$ precursor.

The results of this work indicate that the method of homogeneous doping using $Nb_2O_5:Mg$ precursor can be used to obtain more compositionally homogeneous heavily doped $LiNbO_3:Mg$ single crystals with low coercive field than by direct doping of the melt with magnesium.

Conflict of interest

The authors declare that they have no conflict of interest.

References

[1] M.N. Palatnikov, N.V. Sidorov, O.V. Makarova, I.V. Biryukova. *Fundamental'nye aspekty tekhnologii silno legirovannykh kristallov niobata litiya* (Izd-vo KNTs RAN, Apatity, 2017) (in Russian).

[2] N.V. Sidorov, T.R. Volk, B.N. Mavrin, B.T. Kalinnikov. *Niobat litiya: defekty, photorefraktsiya, kolebatelny spektr, polyaritony* (Nauka, Moskva, 2003) (in Russian).

[3] L.S. Kokhanchik, E.V. Emelin, M.N. Palatnikov. Inorg. Mater., **51** (6), 607 (2015). DOI: 10.1134/S0020168515060084

[4] V.Ya. Shur, A.R. Akhmatkhanov, I.S. Baturin. Appl. Phys. Rew., **2**, 040604 (2015). DOI: 10.1063/1.4928591

[5] V. Kemlin, D. Jegouso, J. Debray, E. Boursier, P. Segonds, B. Boulanger, H. Ishizuki, T. Taira, G. Mennerat, J. Melkonian, A. Godard. Opt. Express., **21** (23), 28886 (2013). https://doi.org/10.1364/OE.21.028886

[6] R.T. Murray, T.H. Runcorn, S. Guha, J.R. Taylor. Opt. Express., **25** (6), 6421 (2017). https://doi.org/10.1364/OE.25.006421

[7] L.A. Bobreva. *Fisiko-khimicheskie osnovy tekhnologiy optichesky vysokosovershennykh nominalno chistykh i legirovannykh nelineynooptycheskikh monokristallov niobata litiya s nizkim effektom fotorefraktsii.* Avtoref. kand. dis. (FGBUN FITs KNTs RAN, Apatity, 2021) (in Russian).

[8] [N.V. Sidorov, L.A. Bobreva, N.A. Teplyakova, M.N. Palatnikov, O.V. Makarova. Inorg. Mater., **55** (11), 1132 (2019). DOI: 10.1134/S0020168519100145]

[9] [M.N. Palatnikov, I.V. Biryukova, O.V. Makarova, N.V. Sidorov, N.A. Teplyakova, S.M. Masloboeva, V.V. Efremov. Inorg. Mater.: Appl. Research, **7** (5), 691 (2016). DOI: 10.1134/S2075113316050208]

[10] [M.N. Palatnikov, I.V. Biryukova, S.M. Masloboeva, O.V. Makarova, O.E. Kravchenko, A.A. Yanichev, N.V. Sidorov. Inorg. Mater. **49** (7), 715 (2013). DOI: 10.1134/S0020168513060083]

[11] [M.N. Palatnikov, S.M. Masloboeva, I.V. Biryukova, O.V. Makarova, N.V. Sidorov, V.V. Efremov. Russ. J. Chem., **59** (3), 178 (2014). DOI: 10.1134/S0036023614030176]

[12] [M.N. Palatnikov, I.V. Biryukova, O.E. Kravchenko, S.M. Masloboeva, O.V. Makarova, V.V. Efremov. Russ. J. Chem., **61** (1), 18 (2016). DOI: 10.1134/S0036023616010186]

[13] M.N. Palatnikov, S.M. Masloboeva, L.G. Arutyunyan, O.E. Kravchenko, I.V. Biryukova, O.V. Makarova, I.N. Efremov, V.T. Kalinnikov. Patent RF № 2012129111/05, 2013 (in Russian).

[14] S. Uda, T. Tsubota. J. Cryst. Growth., **312**, 3650 (2010). DOI: 10.1016/j.jcrysgro.2010.09.052

[15] S. Uda, W.A. Tiller. J. Cryst. Growth., **121** (1–2), 155 (1992). https://doi.org/10.1016/0022-0248(92)90185-L

[16] Yu.K. Voron'ko, A.B. Kudryavtsev, A.A. Sobol, E.V. Sorokin. Trudy IOFAN, **29**, 50 (1991) (in Russian).

[17] Yu.K. Voron'ko, A.B. Kudryavtsev, V.V. Osiko, A.A. Sobol, E.V. Sorokin. Kr. soobsch. po fisike FIAN, (2), 34 (1987) (in Russian).

[18] A.A. Sobol. *Vysokotemperaturnaya spectroskopiya kombinatsionnogo rasseyaniya sveta v tverdykh i rasplavlennykh dielektrikakh.* Avtoref. dokt. dis. (FIAN, M., 2012) (in Russian).

[19] M.D. Fontana, P. Bourson. Appl. Phys. Rev., **2** (4), 040602 (2015). https://doi.org/10.1063/1.4934203

[20] M.N. Palatnikov, O.V. Makarova, N.V. Sidorov. *Rostovye i tekhnologicheskie defekty kristallov niobata litiya razlichnogo khimicheskogo sostava: atlas,* Izd-vo FITs KNTs RAN, Apatity, 2018 (in Russian).

[21] N.V. Sidorov, O.Y. Pikoul, N.A. Teplyakova, M.N. Palatnikov. *Lazernaya konoskopiya i fotoindutsirovannoe rasseyanie sveta v issledovaniyakh svoystv nelineyno-opticheskogo monokristalla niobata litiya* (RAN, M., 2019) (in Russian).

[22] T.C. Damen, S.P.S. Porto, B. Tell. Phys. Rev., **142** (2), 570 (1966). DOI: 10.1103/PhysRev.142.570

[23] N.V. Sidorov, M.N. Palatnikov, N.A. Teplyakova, V.T. Kalinnikov. *Segnetoelektricheskie tverdye rastvory* $Li_xNa_{1-x}Ta_yNb_{1-y}O_3$. *Sintez, struktura, svoystva* (Nauka, M., 2015) (in Russian).

[24] S.M. Masloboeva, N.V. Sidorov, M.N. Palatnikov, L.G. Arutyunyan, P.G. Chufyrev. Russ. J. Chem., **56** (8), 1194 (2011). DOI: 10.1134/S0036023611080183

[25] F. Fayrbroter. *Khimiya niobiya i tantala* (Khimiya, M., 1972) (in Russian).

[26] A.A. McConnell, J.S. Anderson, N.R. Rao. Spectrochimica Acta, **32A** (5), 1067 (1976).
[27] U. Balachandran, N.G. Eror. J. Mater. Science Lett., **1** (9), 374 (1982). DOI: 10.1007/BF00724842
[28] P.S. Dobal, A. Dixit, R.S. Katiyar, H. Choosuwan, R. Guo, A.S. Bhalla. J. Raman Spectr., **33** (2), 121 (2002). DOI: 10.1002/jrs.828
[29] C.N.R. Rao. Ind. J. Pure Appl. Phys., **16**, 227 (1978).
[30] M. Palatnikov, O. Pikoul, N. Sidorov, O. Makarova, K. Bormanis. Ferroelectrics, **436**, 19 (2012). DOI: 10.1080/10584587.2012.730953